Available online at www.sciencedirect.com

ScienceDirect

journal homepage: www.elsevier.com/locate/he

CO tolerant Pt electrocatalysts for PEM fuel cells with enhanced stability against electrocorrosion

Irina Borbáth [a,*], *Kristóf Zelenka* [a], *Ádám Vass* [a], *Zoltán Pászti* [a], *Gábor P. Szijjártó* [a], *Zoltán Sebestyén* [a], *György Sáfrán* [b], *András Tompos* [a]

[a] *Institute of Materials and Environmental Chemistry, Research Centre for Natural Sciences, Hungarian Academy of Sciences Centre of Excellence, Magyar Tudósok körútja 2, H-1117, Budapest, Hungary*

[b] *Institute for Technical Physics and Materials Science, Centre for Energy Research, Konkoly-Thege M. út 29-33, H-1121 Budapest, Hungary*

HIGHLIGHTS

- Composite preparation using 1000 °C pre-treated, HNO_3+glucose functionalized carbon.
- Composites with different $Ti_{0.8}Mo_{0.2}O_2$/C ratios and TiO_2-rutile phase were obtained.
- Moiré pattern from overlapping mixed oxide crystallites in composites was observed.
- Influence of the $Ti_{0.8}Mo_{0.2}O_2$/C ratios of composites on performance was determined.
- Influence of carbon functionalization on the electrochemical performance was studied.

GRAPHICAL ABSTRACT

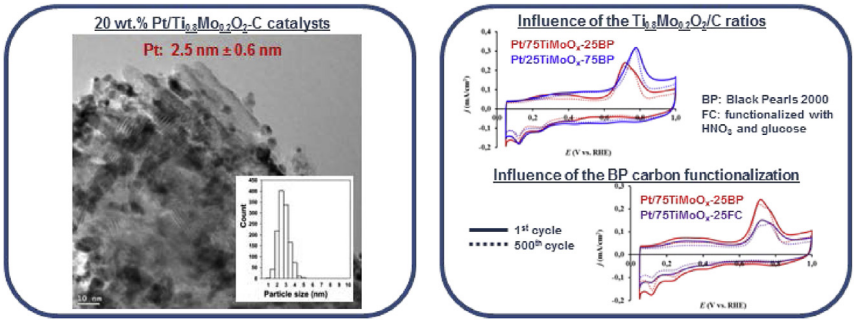

ARTICLE INFO

Article history:
Received 13 February 2020
Received in revised form
24 July 2020
Accepted 1 August 2020
Available online xxx

Keywords:
Functionalized carbon
Glucose
Composite materials
$TiMoO_x$

ABSTRACT

An optimized route for preparation of $Ti_{0.8}Mo_{0.2}O_2$–C composite supports for Pt electrocatalysts with 75/25 and 25/75 oxide/carbon mass ratio was elaborated using commercial (**BP**: Black Pearls 2000) and functionalized (**FC**) carbon materials. The sol-gel-based synthesis resulted in complete Mo incorporation into the rutile-TiO_2 lattice which is a prerequisite for good CO tolerance and high stability. According to the TG and XPS measurements the highest amount of oxygen-containing functional groups was obtained on the BP carbon annealed in nitrogen at 1000 °C and functionalized with HNO_3 and glucose.

The electrochemical stability tests for 500 polarization cycles performed on the 20 wt% Pt/$Ti_{0.8}Mo_{0.2}O_2$–C catalysts revealed similarly small performance loss (8.5–11.8%) in case of all support materials. Considering the negative effect of the oxide content of the catalyst

* *Corresponding author*. H-1519 Budapest, P.O.Box 286, Hungary.
E-mail address: borbath.irina@ttk.hu (I. Borbáth).

https://doi.org/10.1016/j.ijhydene.2020.08.002

0360-3199/© 2020 The Author(s). Published by Elsevier Ltd on behalf of Hydrogen Energy Publications LLC. This is an open access article under the CC BY-NC-ND license (http://creativecommons.org/licenses/by-nc-nd/4.0/).

Please cite this article as: Borbáth I et al., CO tolerant Pt electrocatalysts for PEM fuel cells with enhanced stability against electrocorrosion, International Journal of Hydrogen Energy, https://doi.org/10.1016/j.ijhydene.2020.08.002

Pt electrocatalysts
CO-tolerance

layer on the cell resistance, the catalyst with $Ti_{0.8}Mo_{0.2}O_2$/C = 25/75 ratio was chosen as the most promising.

© 2020 The Author(s). Published by Elsevier Ltd on behalf of Hydrogen Energy Publications LLC. This is an open access article under the CC BY-NC-ND license (http://creativecommons.org/licenses/by-nc-nd/4.0/).

Introduction

Due to their high energy density, low operation temperature, and high conversion efficiency, Polymer Electrolyte Membrane Fuel Cells (PEMFCs) fueled with hydrogen are the most important type of fuel cells for widespread utilization in automobile, stationary and portable applications. One of the key components responsible for the longevity, performance and price of PEMFCs is the electrocatalyst. The best available catalysts belong to the Pt/C family; these are known to suffer from corrosion, which can only be compensated with extremely high Pt loading, keeping the price of the cells high [1–3]. Moreover, CO tolerance of the Pt-based anode catalysts is highly important when feeding low temperature PEMFC stacks with hydrogen obtained from the reforming of hydrocarbons [4]. It is therefore important to explore alternative materials that can provide increased CO tolerance and improved stability across the anticipated potential/pH window compared to carbon [5–8].

According to the literature, the stability of the electrodes can be improved primarily by increasing the stability of the catalyst support. The way for improving the CO tolerance of the electrocatalyst by the bifunctional mechanism is to create interfaces between Pt particles and an oxide-containing support which is (i) stable under the reaction conditions, (ii) electroconductive, (iii) generates OH groups as oxidants at low potential and (iv) stabilizes the small size of the Pt particles [9–12]. Protection against leaching of non-noble metal oxide components under acidic conditions and high potentials is one of the key requirements for fuel cell applications [13,14].

Composite type support materials with TiO_2 coating are widely used. Highly graphitic carbons provide a good backbone for retaining the original nanoscale and uniform TiO_2 coatings (<10 nm) without sintering during heat treatment [15]. Decreasing of the micropore volume in mesoporous carbon by the TiO_2 coating can positively influence the catalytic behavior [16,17]. The strong interaction between the TiO_2 coating on carbon and the Pt results in drastically increased electrochemically active surface area (ECSA) of the Pt and inhibits the agglomeration and corrosion of the metal nanoparticles (NPs) resulting in improved stability in accelerated aging tests [18–20].

However, it is known that high oxide content in the anode catalyst layer can result in some increase of the internal resistance of the cell and as a consequence in a performance loss [21]. Thus, upon the preparation of the oxide-containing composite supports the main goal is to determine an optimal ratio between the oxide and the active carbon in the composites, which provides an oxide coating over carbon, but also ensures the existence of a percolating network of carbon-carbon contacts for guaranteeing the good conductivity of the materials. It is necessary to mention that the literature is somewhat controversial on this question. It appears that the synthesis method used for the preparation of TiO_2 coating over carbon support has the most important influence on the electrochemical properties of the catalysts. Thus, taking into account both the activity and stability of various Pt/TiO_2–C catalysts, in Ref. [22] 40 wt% of TiO_2 in the composite support was chosen as optimal. However, upon investigation of the Pt/TiO_2–C catalysts with different TiO_2 loadings (10, 30 and 60%) the highest stability in the potential range of 0.05–1.3 V (vs. RHE) was obtained on the catalyst with 10% TiO_2 content [23]. Presence of multifunctional mixed oxides in the composite further complicates the situation. It has been demonstrated [24] that if the content of the oxide in the Pt/$Ti_{0.9}Sn_{0.1}O_2$–C catalyst was too low, the promotional role of the $Ti_{0.9}Sn_{0.1}O_2$ was not observed; the highest methanol electrooxidation activity was obtained on the Pt catalysts supported on the composite with a $Ti_{0.9}Sn_{0.1}O_2$/C mass ratio of 15/35. The effect of the carbon content in the C–TaNbTiO$_2$ hybrid support on the physicochemical properties of the Pt–Pd supported catalysts was studied by Wang *et al.* [25]. It has been found that along with excellent electrochemical properties the Pt–Pd catalyst with carbon content of 75 wt% has good conductivity and higher specific surface area compared to the catalyst with 25 wt% of carbon (4.88 S cm^{-1} and 683 m^2 g^{-1} vs. 0.23 S cm^{-1} and 45 m^2 g^{-1}).

In our recent studies [26–29] the design and preparation of Pt electrocatalysts deposited onto $Ti_{(1-x)}M_xO_2$-C (M = W, Mo) composites with $Ti_{(1-x)}M_xO_2$/C = 75/25 and 50/50 wt% content was presented. Optimum experimental conditions were found to synthesize $Ti_{(1-x)}M_xO_2$-C (M = W, Mo; x = 0.2–0.4) composite materials with exclusive incorporation of the W or Mo ions into substitutional sites of the TiO_2-rutile lattice. Under such circumstances the TiO_2 lattice protects the doping metals from dissolution, while the incorporated dopants can still provide CO tolerance. We demonstrated that the catalytic properties of the system are mainly determined by the interaction between Pt and doping transition M metals (M = W, Mo). The electrochemical stability tests revealed that the degradation rate of the composite supported catalysts is much smaller than that of the Pt/C and PtRu/C [26,27,30]. Better performance of the Pt/$Ti_{0.7}M_{0.3}O_2$–C (M = W, Mo) catalysts in a single cell test device using hydrogen containing 100 ppm CO compared to the reference Pt/C and PtRu/C catalysts was also demonstrated [31].

In principle, in order to improve dispersion of Pt NPs, or any other metallic species catalytically active in a given (electro)catalytic reaction, it would be advantageous to

Please cite this article as: Borbáth I et al., CO tolerant Pt electrocatalysts for PEM fuel cells with enhanced stability against electrocorrosion, International Journal of Hydrogen Energy, https://doi.org/10.1016/j.ijhydene.2020.08.002

utilize supports with large surface area displaying a high number of functional groups. It is well known that the inert surface of carbon requires suitable chemical modification to increase its hydrophilicity and, additionally, to improve the interaction between the support surface and the active phase. Thus, functionalization of the carbonaceous support may help a more disperse deposition of metal oxides [32].

Common procedure of the surface functionalization of the carbon support consists of treatment with HNO_3, H_2O_2, a mixture of HNO_3–H_2SO_4 acids, citric acid, etc. [33–40]. Torres *et al.* [41] showed that the effect of the different oxidants can be related to the nature of the functional groups on the carbon surface. Thus, HNO_3-treated carbon displays a high density of both strong and weak acid sites, while H_2O_2-treated carbons show an important concentration of weak acid sites along with a low concentration of strong acid sites [41,42].

It has been demonstrated that functionalization of the carbonaceous support with glucose, HNO_3 or mixture of HNO_3–H_2SO_4 acids facilitates the growth of uniform layer of very small TiO_2 NPs on the carbon surface [43,44]. The use of adsorbed glucose is a good tool to control the size of the deposited TiO_2 NPs providing homogeneous coating and to enhance conductivity of TiO_2/C composite [45]. Recent results obtained on Pt/TiO_2/C catalysts, prepared using glucose-treated Vulcan XC-72, show superior oxygen reduction reaction (ORR) activity and better durability during accelerated stress tests [46]. It is necessary to mention that in our previous studies upon the preparation of $Ti_{(1-x)}Mo_xO_2$-C composite materials [28–31] carbon was used without preliminary functionalization.

In the present work our aim is to develop a synthesis method for composite supports based on $Ti_{0.8}Mo_{0.2}O_2$-coated functionalized carbon, to assess the potential beneficial effect of the functionalized carbon on the electrocatalytic behavior and stability of the 20 wt% Pt/$Ti_{0.8}M_{0.2}O_2$–C catalysts and to determine the optimal $Ti_{0.8}Mo_{0.2}O_2$/C ratio for retaining of the stable TiO_2-based coating over carbon during the stability test.

Materials and methods

Functionalization of commercial carbon

The functionalization of commercial carbon (BP: Black Pearls 2000 (Cabot)) was done using either a one-step treatment with glucose or by a two-step treatment with HNO_3 and glucose (HNO_3 + glucose) according to the procedure recommended by Odetola *et al.* [43,46], demonstrated schematically in Figs. S1 and S2 of the Supplementary Material.

In some cases before functionalization carbon was pretreated in nitrogen at 1000 °C (BP1000). Occasionally, previously functionalized carbon was annealed at 500 °C in N_2 for elimination of less stable surface oxygen groups. Details of such treatments are given in the Supplementary Material.

Synthesis of $Ti_{0.8}Mo_{0.2}O_2$–C composite materials and Pt electrocatalysts

Using these functionalized carbon (FC) materials and unmodified BP carbon the synthesis of mixed-oxide coated $Ti_{0.8}Mo_{0.2}O_2$–C composites (atomic ratio Ti/Mo = 80/20) with the $Ti_{0.8}Mo_{0.2}O_2$/C mass ratio of 75/25 was done as described earlier in our previous studies (see Fig. 1, route A). Shortly, the synthesis consists of three main steps: low temperature deposition of rutile nuclei on the carbon backbone, which is completed by an aging step, introduction of the Mo precursor and driving the Mo into the rutile crystallites by a high-temperature annealing step. For further details see our earlier works [28–30].

Upon the preparation of the composites with higher carbon content ($Ti_{0.8}Mo_{0.2}O_2$/C = 25/75) after addition of carbon to the TiO_2 sol appropriate amount of cc. HNO_3 was also added to compensate the whole acidity of the synthesis mixture (see Table 1 and Fig. 1, route B).

Our preliminary results demonstrate that upon preparation of the composite materials with the $Ti_{0.8}Mo_{0.2}O_2$/C = 25/75 ratio the aging of the synthesis mixture at room temperature (RT) for 4 days results in the formation of pure TiO_2-anatase phase, which is not suitable for Mo doping with our technique. Therefore as shown in Fig. 1 (route B), for the formation of the TiO_2-rutile phase on the carbon surface, the 4-day aging procedure was divided into two additional steps: (i) stirring at RT for 88 h and (ii) raising the temperature to 65 °C and holding at 65 °C for another 8 h.

The difference between the preparation of composite materials with different $Ti_{0.8}Mo_{0.2}O_2$/C ratios was presented in Table 1 and Fig. 1.

In the following discussion the sample identifier contains the nominal composition of the composite materials denoted by the nominal weight percentage of the carbon with respect to the mixed oxide content, along with the type of carbon used, as 25BP (meaning the composite of 75 wt% of $Ti_{0.8}Mo_{0.2}O_2$ and 25 wt% of untreated Black Pearls 2000 carbon) or 25FC and 75BP or 75FC, respectively; in all cases the desired Ti/Mo atomic ratio was 80/20.

Loading of 20 wt% of Pt using H_2PtCl_6 precursor compound was done by $NaBH_4$ and ethylene glycol reduction-precipitation method as described in details in Refs. [28–30].

Physicochemical characterization

Surface functionalization of the carbon was followed by thermogravimetric and XPS measurements. The composite materials and the corresponding Pt catalysts were characterized by XRD, TEM, XPS and nitrogen adsorption measurements.

Thermogravimetric (TG) measurements were done using a modified PerkinElmer TGS-2 thermobalance. About 3 mg samples were measured in inert argon atmosphere at a flow rate of 140 ml/min. The samples were heated at a rate of 20 °C/min from room temperature to the final temperature of 900 °C in a platinum sample pan.

Please cite this article as: Borbáth I et al., CO tolerant Pt electrocatalysts for PEM fuel cells with enhanced stability against electrocorrosion, International Journal of Hydrogen Energy, https://doi.org/10.1016/j.ijhydene.2020.08.002

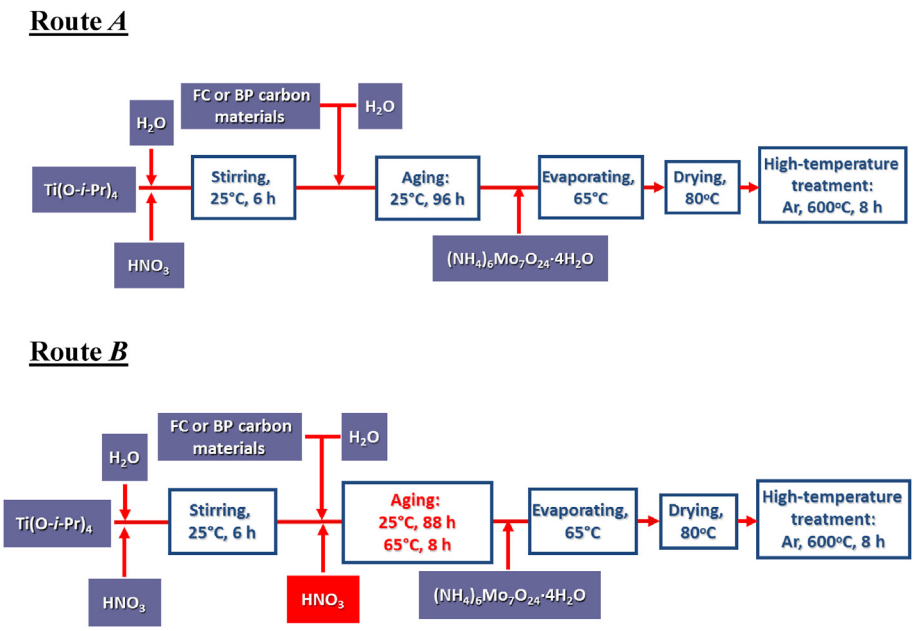

Fig. 1 – Flow chart for preparing 75%$Ti_{0.8}Mo_{0.2}O_2$–25%C (route A) and 25%$Ti_{0.8}Mo_{0.2}O_2$–75%C (route B) composite materials using functionalized carbon (FC) and unmodified BP carbon materials. Difference between the synthesis routes are highlighted in red color. (For interpretation of the references to colour in this figure legend, the reader is referred to the Web version of this article.)

Table 1 – Nominal composition and preparation details of the samples with the different $Ti_{0.8}Mo_{0.2}O_2$/C ratios.

Samples nominal composition[a]	TiO_2 sol			Suspension of carbon			Mo precursor, g[c]
	H_2O, mL	HNO_3, mL	Ti precursor, mL[b]	C, g	H_2O, mL	HNO_3, mL	
75$Ti_{0.8}Mo_{0.2}O_2$–25C	21	2.35	2.05	0.25	10	–	0.2989
25$Ti_{0.8}Mo_{0.2}O_2$–75C	7	0.78	0.68	0.75	15	0.78	0.0997

[a] Expected composition of composites with different $Ti_{0.8}Mo_{0.2}O_2$/C mass ratio.
[b] Ti precursor compound: titanium-isopropoxide (Ti(O-*i*-Pr)$_4$, Aldrich, 97%).
[c] Mo precursor compound: ammonium heptamolybdate tetrahydrate $(NH_4)_6Mo_7O_{24} \times 4H_2O$, Merck, 99%). HNO_3 (65%, Molar Chemicals, a.r.).

X-ray photoelectron spectroscopy (XPS) studies were performed in an Omicron EA 125 electron spectrometer. Non-monochromatized MgKα (1253.6 eV) radiation was used for excitation, while spectra were collected in the "Fixed Analyser Transmission" mode (E_{pass}: 30 eV, resolution around 1 eV). In order to prepare samples with appropriate mechanical stability and electrical conductivity, the powders were suspended in hexane and drops of the suspensions were dried onto standard stainless steel Omicron sample plates. Measured data were analyzed by the CasaXPS [47] and the XPSMultiQuant [48,49] software packages.

Powder X-ray diffraction (XRD) studies were done using a Philips model PW 3710 based PW 1050 Bragg-Brentano parafocusing goniometer with CuKα radiation (λ = 0.15418 nm), graphite monochromator and proportional counter.

Transmission Electron Microscopy (TEM) studies of the samples were made by use of a JEOL 3010 high resolution transmission electron microscope operating at 300 kV.

Nitrogen adsorption measurements were used to determine the specific surface area (S_{BET}). Prior to the measurement the sample was pretreated in He flow at 750 °C for 8 h then evacuated at 10^{-6} Torr and cooled down to the temperature of liquid nitrogen.

Electrochemical characterization

The electrochemical measurements were carried out in a standard three-electrode configuration at RT using a Bio-logic SP150 potentiostat. 0.5 M H_2SO_4 was used as electrolyte. Glassy carbon (GC; d = 0.3 cm) electrode with 0.0707 cm^2 surface area was used as working electrode. Platinum wire was used as counter electrode and a hydrogen electrode as reference electrode. All potentials are given on RHE scale.

Electrocatalytic performance of the 20 wt% Pt/$Ti_{0.8}Mo_{0.2}O_2$–C electrocatalysts was studied by cyclic voltammetry and CO_{ads}-stripping voltammetry measurements combined with stability test involving 500 polarization cycles and the second CO_{ads}-stripping voltammetry measurement. The details of the working electrode preparation, the catalyst ink composition and electrocatalytic measurements were described in Refs. [28–30].

Please cite this article as: Borbáth I et al., CO tolerant Pt electrocatalysts for PEM fuel cells with enhanced stability against electrocorrosion, International Journal of Hydrogen Energy, https://doi.org/10.1016/j.ijhydene.2020.08.002

Results and discussion

Functionalization of commercial carbon

Functionalization of the carbon has been done to reach a more disperse deposition of metal oxides over the carbon support. Thermal analysis is a straightforward method for assessing the nature of the introduced functional groups. Table 2 summarizes the functionalized carbon materials and their functional group content based on TG measurements as well as the BET surface area of the $Ti_{0.8}Mo_{0.2}O_2$–C composites with 25 wt% carbon content. As shown in Table 2 after treatment with glucose, an –OH rich molecule, or with (HNO_3 + glucose) the content of the surface oxygen groups in FCs was estimated between 9.4 and 19.5%, respectively. Pre-treatment of carbon in nitrogen at 1000 °C for 3 h before functionalization (BP1000) results in further increase of the amount of oxygen-containing functional groups up to 22%.

As shown in Fig. 2 the thermal decomposition of FCs proceeds with elimination of the surface functional groups in one (sample FC-1) or two steps (sample FC-2). Upon TG measurements done on glucose-doped carbon materials the mass losses observed at temperature below 500 °C were assigned to the pyrolysis of glucose, which proceeds with elimination of water and volatile decomposition products [43,46,50–52].

Moreover, it has been reported [53,54] that stronger acid groups (e.g. carboxylic, anhydride groups) decompose between 200 and 500 °C with maximum at 273 °C, whereas the decomposition of the weaker acid sites (e.g. lactone, phenol, carbonyl groups) started at higher temperatures (407 °C).

According to the TG results (see Table 2 and Fig. 2) it can be argued that the amount and type of the surface oxygen groups depends on the type of the oxidizing/functionalizing reagent used.

However, it is well known that catalysts supported on FC could not tolerate high-temperature treatments (HTT, an essential step in the synthesis of the mixed oxides), due to the instability of surface oxygen groups of the support [55]. Thus, even if these surface groups help in ensuring high dispersion of deposited metal or metal oxide, sensitivity of the functional groups to the HTT negatively influences the final dispersion of metallic Pt and its resistance to sintering if the preparation of the catalyst requires annealing at elevated temperatures. In this respect, the final dispersion of deposited metal or metal oxides and resistance to sintering are more negatively affected by the presence of the less stable functional groups. To resolve this problem prior to the introduction of the active phase the elimination of the surface functional groups, which decompose at low temperature, was recommended using HTT in He at 500 °C for 1 h [56,57].

Since for incorporation of Mo into the rutile-TiO_2 lattice HTT at 600 °C is needed [28–30], we checked the effect of the recommended pre-annealing treatment on the functional group content of the FC-2 material. Accordingly, sample FC-2 was annealed in N_2 at 500 °C for 1 h. As shown in Fig. 2 using this pre-treatment the surface groups, which decomposed below 500 °C, were indeed removed (sample FC-2/500), but during this treatment the major part of the functional groups (65%) was eliminated (see Table 2). Because of the quite small amount of the remaining functional groups, for the preparation of the mixed oxide coating over carbon this pre-annealing step was omitted.

The results of the BET surface area measurements of the 25FC composite materials were also included in Table 2. As shown in Table 2, previous treatment of carbon at 1000 °C before functionalization does not lead to decrease of the S_{BET} values of the composite support materials. According to the BET measurements all composites studied have proper specific surface area required for fuel cell electrocatalysts (>100 m^2/g).

XPS studies were done using functionalized carbon materials FC-3 and FC-4 with highest amount of functional groups. Composition data (in atom%) are summarized in Table 3.

The successful functionalization is indicated by the enhanced oxygen content of the FC-3 and FC-4 samples. In addition, a small amount of N and S (close to the detection limit) were also generally found in the samples.

The analysis of the C 1s and O 1s line shapes allows the tentative identification of the functional groups introduced by the functionalization. For this, the C 1s and O 1s spectrum of the BP sample pre-treated at 1000 °C was used as reference; differences with respect to the reference line shape arise as a result of appearance of new functional groups. The C 1s and O 1s spectra for the studied carbon materials are shown in Fig. 3. For identification of the carbon and oxygen chemical states, the general XPS databases [58,59] and several other works [60,61] were used.

The C 1s spectrum measured on the annealed BP1000 active carbon material shows the somewhat asymmetric peak shape characteristic for graphitic carbon. The main component is at 284.4 eV which corresponds to the binding energy reported for graphitic materials; the loss peak arising due to the excitation of the delocalized electron system at around 6 eV higher binding energy is also evident. In case of the FC samples, in addition to the graphitic line shape deduced from the spectrum of the annealed BP material, two new peaks are needed for adequate fitting of the measured data. One of them appears around 286.3 eV binding energy. Literature assigns this component to carbon species singly bound to oxygen

Table 2 – Structural properties of the FCs detemined by TG measurements and the BET surface area of the 25FC composite materials.

Sample	Treatment[a]	FG, %[b]	S_{BET}, m^2/g[c]
FC-1	BP/glucose	9.4	141
FC-2	BP/HNO_3 + glucose	19.5	135
FC-2/500	**FC-2,** N_2, 500 °C, 1 h[d]	6.9	123
FC-3	BP1000[e]/glucose	17.4	169
FC-4	BP1000[e]/HNO_3 + glucose	22.0	147

[a] Functionalization treatment of commercial BP carbon.
[b] The percentage of the surface oxygen functional groups (**FG**) in FCs estimated from TG results based on the starting weight of functionalized materials and carbon residues measured at 900 °C after the thermal decomposition.
[c] BET surface area of the 25FC composite materials prepared on the given functionalized carbon.
[d] Additional treatment of the sample FC-2 in N_2 at 500 °C for 1 h.
[e] BP carbon pretreated at 1000 °C in nitrogen for 3 h before functionalization.

Please cite this article as: Borbáth I et al., CO tolerant Pt electrocatalysts for PEM fuel cells with enhanced stability against electrocorrosion, International Journal of Hydrogen Energy, https://doi.org/10.1016/j.ijhydene.2020.08.002

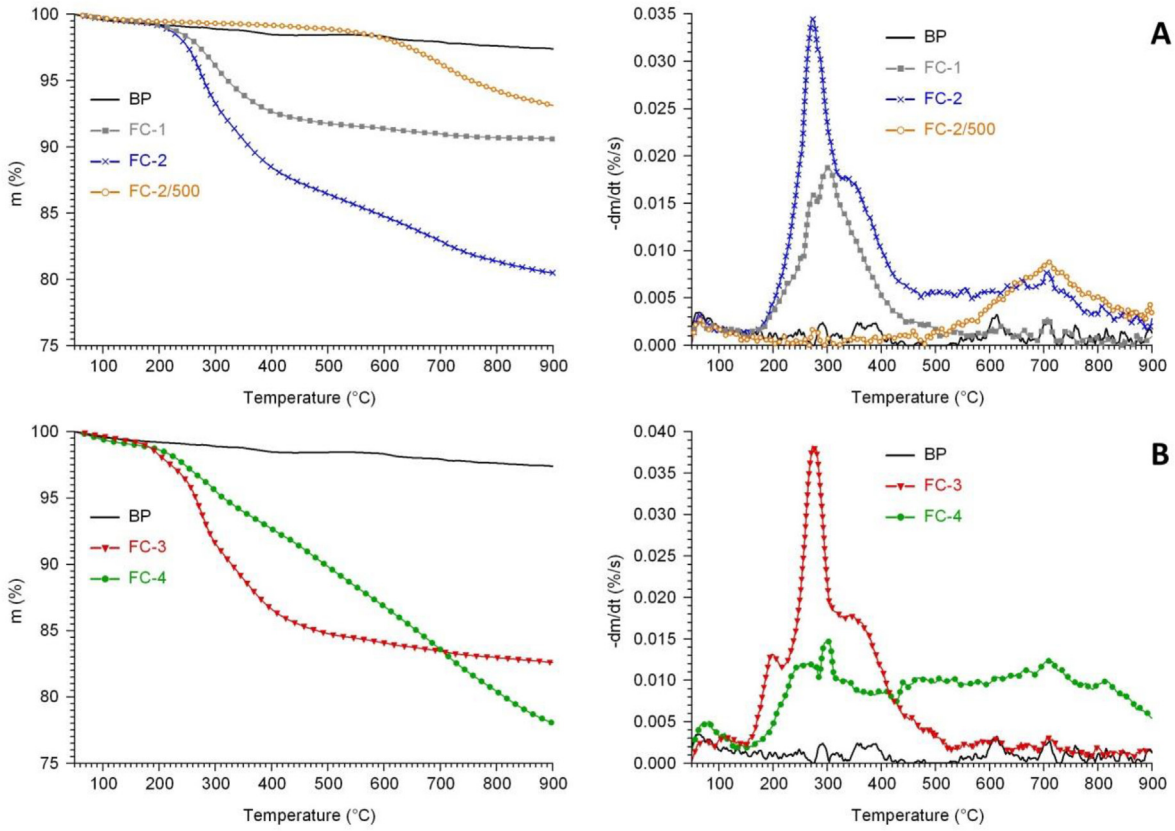

Fig. 2 – TG and DTG curves of the functionalized carbon materials: (A) FC-1, FC-2 and FC-2/500 prepared using additional treatment of the sample FC-2 in N_2 at 500 °C for 1 h. (B) FC-3 and 4- FC-4. Results obtained on unmodified BP carbon were given for comparison.

Table 3 – Composition of the annealed active carbon (BP) and its functionalized derivatives (FCs) from XPS measurements (atom%).

Sample	C	O	N	S
BP1000	98.0	1.5	0.3	0.2
FC-3	94.7	5.1	–	0.2
FC-4	89.9	9.8	0.3	–

[60,61] such as a C–OH bond or C–O–C type carbon-oxygen connections in epoxide or lactone groups. The other is found around 288.5 eV binding energy and can be assigned to more highly oxidized carbon species such as carboxylic or anhydride functionalities or carbon atoms bound to more than one oxygen atom in lactones.

According to the presented spectra, the functionalities introduced by the glucose treatment (FC-3) are mainly carbon atoms singly bound to oxygen (2–3% of the total carbon content), while the amount of more heavily oxidized carbon atoms remains low (1% of the carbon content). In case of the HNO_3-treated and glucose-functionalized FC-4 sample the amount of the C atoms singly bound to oxygen remained around 2%, while the contribution from the more strongly oxidized carbon species increased to 3%.

The O 1s spectra confirm the above observations. A relatively small amount of oxygen was found in the pre-annealed BP1000 carbon material; its O 1s spectrum was modeled by three weak contributions. The one observed around 531.4 eV can be ascribed to epoxide groups, the one around 533.5 eV may be due to carboxylic, lactone or ether groups while the very weak signal around 535 eV is from adsorbed water molecules [60,61].

Using the O 1s spectrum of the BP1000 material as a baseline reference, three further contributions can be identified in the spectrum of the glucose-treated FC-3 sample. There is a weak low binding energy component around 530.5 eV, which arises from oxygen atoms with double bond to a carbon atom. A similarly weak contribution around 533.0 eV indicates the appearance of new carboxylic or lactone groups after functionalization. However, the main O 1s component is a peak at 532.4 eV, which can be ascribed to oxygen singly bound to carbon such as in C–OH groups. Thus, both the C 1s and the O 1s data confirm that the glucose functionalization mainly increased the amount of C–OH groups, although more oxidized carbon species were also formed in a small amount.

In case of the FC-4 sample the O 1s spectrum indicates that a wide range of carbon-oxygen connections were formed. The low binding energy peak at 530.6 eV became more intense than after the glucose functionalization (FC-3 sample), suggesting the increase of the amount of carbonyl-like species. A strong peak around 531.6 eV indicates the considerable number of epoxide groups. The amount of hydroxyl groups must be smaller than after the glucose functionalization, as the corresponding peak at 532.5 eV is relatively weaker. A

Please cite this article as: Borbáth I et al., CO tolerant Pt electrocatalysts for PEM fuel cells with enhanced stability against electrocorrosion, International Journal of Hydrogen Energy, https://doi.org/10.1016/j.ijhydene.2020.08.002

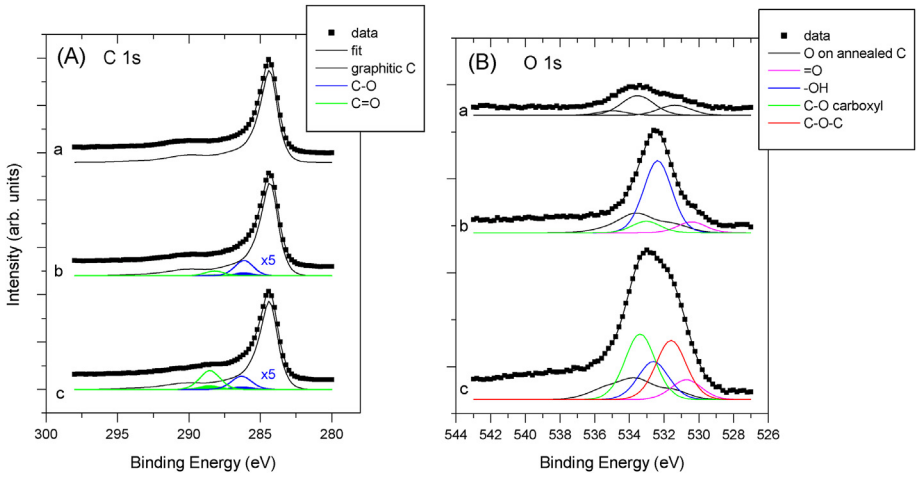

Fig. 3 – (A): C 1s and (B): O 1s spectra of the (a): BP pre-treated at 1000 °C (BP1000), (b) glucose-functionalized BP1000 (FC-3) and (c): HNO_3-treated and glucose-functionalized BP1000 (FC-4) samples. O 1s spectra were normalized to the corresponding C 1s spectra so the relative intensity of the O 1s spectra correlates with the oxygen content of the materials. In panel (A) the components arising after functionalization are shown in their original intensity (filled curves) and after multiplication by 5 (for better visibility, unfilled curves).

strong component at 533.3 eV suggests that numerous carboxylic, lactone or ether groups were formed as the result of the treatment.

Characterization of the $Ti_{0.8}Mo_{0.2}O_2$–C composite materials and related Pt catalysts

Physicochemical characterization

As one of our aims is to check the effect of the functional groups on the nature and the electrochemical behavior of the composites and the electrocatalysts deposited onto them, we present here further data obtained on composite supports and catalysts prepared using FC-4 with the highest content of oxygen-containing functional groups of different character, in comparison with data for non-functionalized BP-based systems.

Fig. 4 shows the XRD patterns measured before and after HTT on $Ti_{0.8}Mo_{0.2}O_2$–C composites with different $Ti_{0.8}Mo_{0.2}O_2$/C ratios prepared using FC-4 and unmodified BP carbon. As shown in Fig. 4A–D in all investigated samples (i) only the reflections of the TiO_2-rutile crystallites were present; (ii) no changes in the lattice parameters connected to the degree of Mo incorporation were observed (all diffractograms indicated $a = 4.640$ Å, $c = 2.935$ Å; the deviation from the values of pure rutile ($a = 4.593$ Å, $c = 2.959$ Å) can be used to assess the extent of Mo doping [28]) and (iii) no reflections characteristic to MoO_2 or MoO_3 were found. These results are in good agreement with our previous studies which demonstrated that the Ti/Mo atomic ratio of 80/20 in the $Ti_{(1-x)}Mo_xO_2$-C ($x = 0.2–0.4$) composite materials is an optimum having total Mo incorporation into the rutile-TiO_2 lattice, which ensures high stability of the $Ti_{0.8}Mo_{0.2}O_2$–C composite [28,30]. Accordingly, the composite with Ti/Mo = 80/20 atomic ratio was chosen to study the effect of the functionalization and $Ti_{0.8}Mo_{0.2}O_2$/C ratio on the activity and stability of Pt electrocatalysts.

The less sharp diffraction peaks observed in the XRD pattern of the samples with low mixed oxide content in the carbon matrix (75BP and 75FC-4) as compared to 25BP and 25FC-4 samples may be attributed to the small mixed oxide content in the composite materials (see Fig. 4B and D).

Deposition of platinum resulted in the appearance of characteristic reflections at 2 theta values of 39.6, 47.4, 67.1°, corresponding to the (111), (200), and (220) reflections of the fcc structure of platinum, respectively [12,62] (Fig. 4, green curves). The broad line shape of Pt indicates very small crystallites.

The apparent surface composition of the composites prepared on untreated or functionalized carbon with different oxide/carbon ratios were determined by XPS and are summarized in Table 4.

A general and repeatedly observed feature of the composites prepared on the untreated BP carbon is that the apparent mixed oxide content is always notably smaller than the nominal value. It is explained by a somewhat inhomogeneous nature of the mixed oxide coating, containing also several larger crystallites; under such circumstances XPS tends to underestimate the amount of the oxide [28]. Nevertheless, the $Ti_{0.8}Mo_{0.2}O_2$/C ratio of the composite prepared on the functionalized carbon is clearly closer to the nominal value, which suggests a change in the structure of the composite towards a more disperse and a more homogeneous oxide coating over the carbon. At the same time, as shown in Table 4 the Ti/Mo ratio seems to depend on the mixed oxide content but not on the type of the carbon used.

The BET surface area of the composite support materials with different $Ti_{0.8}Mo_{0.2}O_2$/C ratios prepared using the BP and FC-4 carbons was presented in Table 5 (results of nitrogen adsorption measurements were presented in Table S1 and Fig. S3 of the Supplementary Material). High values of the S_{BET} obtained on our composite materials comparing to low values generally characteristic for pure oxides demonstrate that in the presence of carbon the particles of the composite materials are successfully protected from sintering.

Please cite this article as: Borbáth I et al., CO tolerant Pt electrocatalysts for PEM fuel cells with enhanced stability against electrocorrosion, International Journal of Hydrogen Energy, https://doi.org/10.1016/j.ijhydene.2020.08.002

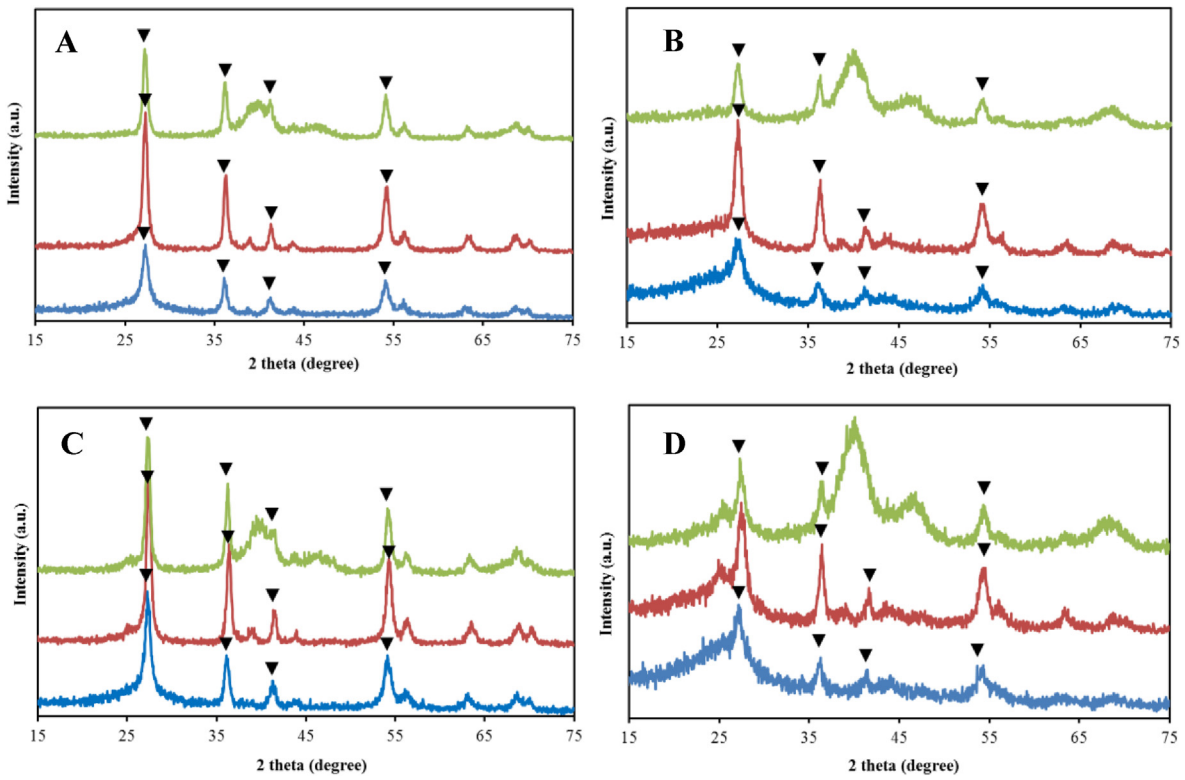

Fig. 4 – XRD patterns of $Ti_{0.8}Mo_{0.2}O_2$–C composites before HTT (blue), after HTT (red) and after Pt loading (green). Samples with different $Ti_{0.8}Mo_{0.2}O_2$/C ratios prepared using BP and FC-4 carbon: 25BP (A); 75BP (B); 25FC-4 (C); 75FC-4 (D). ▼- Rutile. (For interpretation of the references to colour in this figure legend, the reader is referred to the Web version of this article.)

Table 4 – Composition of the mixed oxide–carbon composite supports determined by XPS measurements.

Sample	Ti/Mo (at%/at%)[a]	(Ti + Mo + O)/C (wt%/wt%)[b]
25FC-4	3.6/1	70/30
25BP	3.5/1	58/42
75FC-4	5.2/1	20/80
75BP	4.9/1	19/81

[a] The nominal Ti/Mo ratio = 4/1.
[b] The nominal composition of the support: 75 wt% $Ti_{0.8}Mo_{0.2}O_2$ - 25 wt% C for the 25C materials and 25 wt% $Ti_{0.8}Mo_{0.2}O_2$ - 75 wt% C for the 75C composites (C= FC-4 or BP).

Table 5 – Influence of the functionalization treatment of carbon and the $Ti_{0.8}Mo_{0.2}O_2$/C ratio in composite materials on the structural properties and electrochemical performance of the corresponding Pt electrocatalysts.

Sample	S_{BET}, m^2/g[a]	Pt size, nm (TEM)[b]	$E_{CO,max}$,[c] mV	ECSA, m^2/g_{Pt}	Δ ECSA, %[d]
Pt/25BP	248	2.9 ± 0.8	705 (*sh*: 745)	81.6 ± 8.4	9.1
Pt/75BP	1120	2.7 ± 0.7	775	69.1 ± 2.1	11.8
Pt/25FC-4	147	2.5 ± 0.6	705 (*sh*: 745)	60.9 ± 4.5	11.0
Pt/75FC-4	726	2.8 ± 0.7	775	65.4 ± 6.1	8.5

[a] Specific surface area of the composite support materials.
[b] Particle size determined by measuring the diameters of no less than 1000 randomly selected metal particles in at least ten micrographs of each sample taken from non-aggregated areas using ImageJ software.
[c] The position of the main CO stripping peak measured on fresh catalysts.
[d] Δ ECSA = {1-($ECSA_{500}$/$ECSA_1$)} × 100%; ***sh*** = shoulder.

As follows from Table 5 (i) the increase of the carbon content in the composite materials (75BP and 75FC-4) results in pronounced increase of the S_{BET}; (ii) surface area of the FC-containing supports is lower compared to the composites prepared using unmodified BP carbon; (iii) the lowest value of the S_{BET} = 147 m^2/g was obtained on the 25FC-4 composite containing high amount of mixed oxide. The decrease of the S_{BET} of the composites prepared using FCs, independently of the content of carbonaceous material, can be an indication of the formation of more homogeneous mixed-oxide coating compared to the samples prepared using unmodified BP.

TEM images of the electrocatalysts prepared using FC-4 and BP carbons are presented in Figs. 5 and 6. The Pt particle size values determined from TEM experiments are given in Table 5. In all samples studied a good dispersion of the Pt particles was observed.

The difference observed between TEM images of composite materials with high (Fig. 5) and low content of mixed oxide (Fig. 6) is quite pronounced. The presence of the Moiré pattern (Figs. 5B,D and 6B) arising from overlapping mixed oxide

Please cite this article as: Borbáth I et al., CO tolerant Pt electrocatalysts for PEM fuel cells with enhanced stability against electrocorrosion, International Journal of Hydrogen Energy, https://doi.org/10.1016/j.ijhydene.2020.08.002

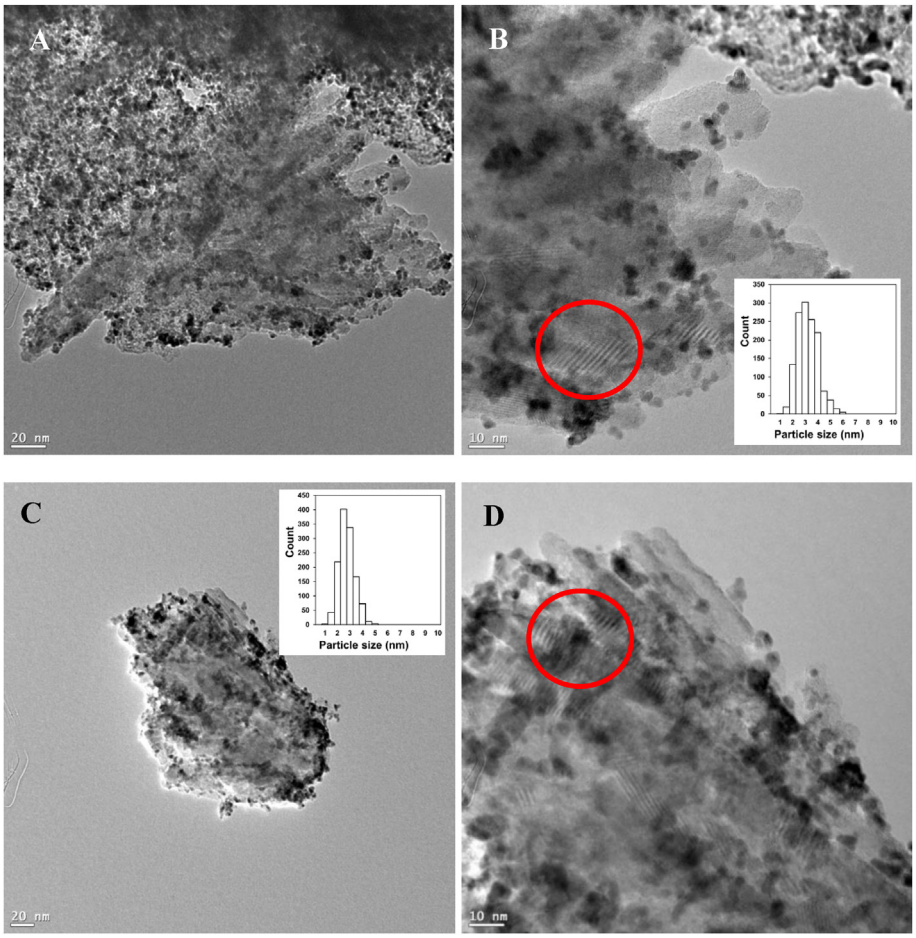

Fig. 5 – TEM images and corresponding histograms of particle size distribution for the Pt/25BP (A, B) and Pt/25FC-4 (C, D) catalysts; characteristic Moiré pattern was marked with red circle. (For interpretation of the references to colour in this figure legend, the reader is referred to the Web version of this article.)

crystallites in the composite materials with high mixed oxide content confirmed the success of TiO_2-based coating formation over the carbon. Even spatial distribution of oxide crystallites suggested that a quite homogeneous coverage was achieved. At the same time, in case of the unmodified carbon based composite, the large, nanorod-like mixed oxide rutile crystallites mentioned above are also visible (Fig. 5A), while a more homogeneous mixed oxide structure is observed in case of the FC-based support (Fig. 5C).

As seen from Fig. 6 in the samples with high content of carbonaceous materials the presence of the oxide layers over carbon was less obvious. These results are in a good agreement with our previous observations obtained on the composites with mixed oxide/carbon mass ratio of 50/50 [26,27,31].

Our preliminary assumption was that by increasing the functional group density, we can modify the nucleation and growth of the rutile-TiO_2 phase, which may have some beneficial effect on the coverage of the mixed oxide over the carbonaceous backbone. This assumption was based on literature results [43–46], and the physicochemical characterization results indeed demonstrate that our efforts for better mixed oxide coverage were at least partly successful by using the functionalization treatment.

Electrochemical performance

The influence of the functionalization treatment of carbon and the $Ti_{0.8}Mo_{0.2}O_2$/C ratio in composite materials on the electrochemical performance of the catalysts was demonstrated in Table 5 and Figs. 7 and 8.

The voltammograms show the general characteristics observed previously for the $Ti_{0.8}Mo_{0.2}O_2$–C composite supported electrocatalysts [28–30]. The cyclic voltammograms contain two notable regions: the adsorption/desorption peaks of under-potentially deposited hydrogen (between 50 and 400 mV) and a peak pair between 380 mV and 530 mV assigned to reduction/oxidation of surface Mo species. The appearance of these redox peaks in the voltammograms confirms the Pt–Mo interactions, which is a characteristic feature for the catalysts containing Pt and Mo in close vicinity [29,63,64].

The CO_{ads} stripping voltammograms contain the so-called pre-peak region starting at 50 mV, which is due to Mo-assisted oxidation of weakly bound CO species on Pt and is an indicator of the CO tolerance of the catalysts. These features demonstrate that all systems, regardless to the functionalization treatment of the carbon or to the mixed oxide/carbon ratio, contain active Pt species closely associated to surface Mo ions

Please cite this article as: Borbáth I et al., CO tolerant Pt electrocatalysts for PEM fuel cells with enhanced stability against electrocorrosion, International Journal of Hydrogen Energy, https://doi.org/10.1016/j.ijhydene.2020.08.002

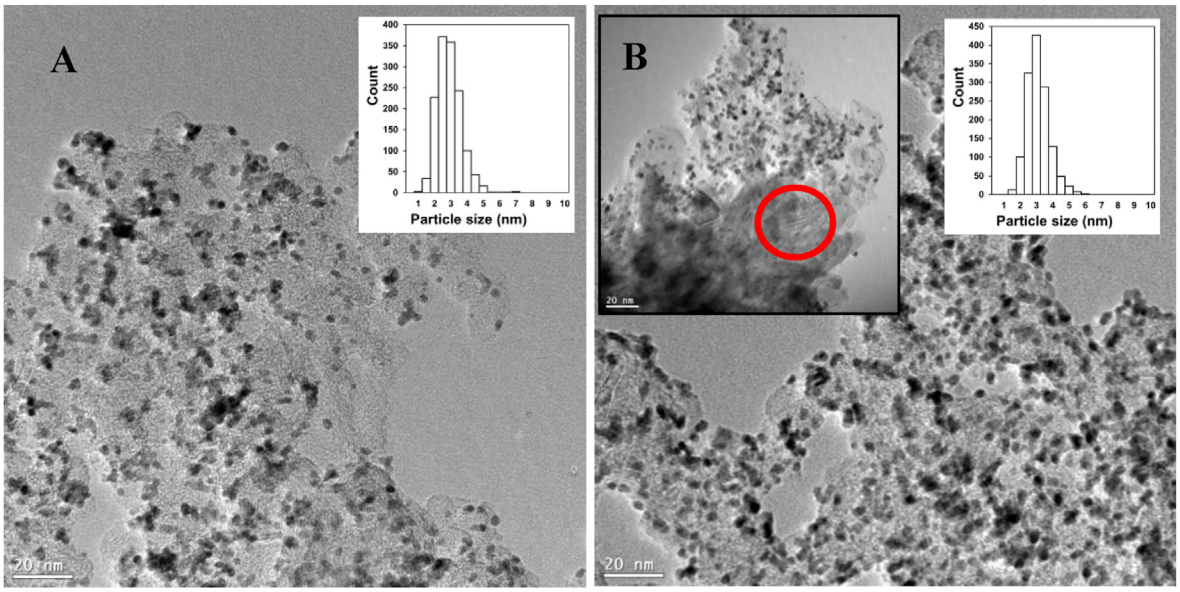

Fig. 6 – TEM images and corresponding histograms of particle size distribution for the Pt/75BP (A) and Pt/75FC-4 (B) catalysts. The insert in B shows a micrograph of the same sample with a larger agglomeration of the surface oxide; characteristic Moiré pattern was marked with red circle. (For interpretation of the references to colour in this figure legend, the reader is referred to the Web version of this article.)

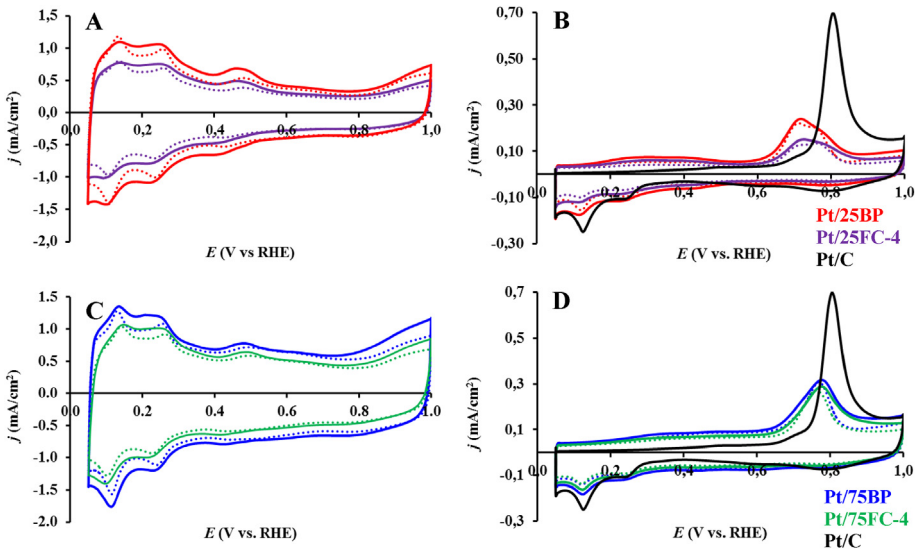

Fig. 7 – Influence of the previous functionalization of active carbon on the electrochemical performance of the composite supported Pt catalysts. Cyclic voltammograms (A, C) and CO_{ads} stripping voltammograms (B, D) of the electrocatalysts recorded in 0.5 M H_2SO_4 before (solid curves) and after 500 cycles (dotted curves) of the stability test. Catalysts (A, B) with low carbon content (Pt/25BP (red), Pt/25FC-4 (violet)) and (C, D) with high carbon content (Pt/75BP (blue), Pt/75FC-4 (green)); the CO_{ads} stripping voltammogram obtained on the fresh reference 20 wt% Pt/C catalyst (black) is given for comparison. Sweep rate: 100 mV/s (A, C) and 10 mV/s (B, D). (For interpretation of the references to colour in this figure legend, the reader is referred to the Web version of this article.)

in the support. The shape of the CO_{ads} stripping voltammograms and the position of the main CO_{ads} stripping peak mainly depend on the mixed oxide content and are independent on the type of carbonaceous material used for composite material preparation (FC or BP). The position of the main CO_{ads} stripping peak on the Pt/25BP and Pt/25FC-4 catalysts (705 mV) is shifted towards less positive potentials by 70 mV with respect to the main peak observed on the Pt/75BP and Pt/75FC-4 samples with high carbon content (775 mV), thus demonstrating increased tolerance to CO of the catalysts with high mixed oxide content. After 500 cycles of the stability test the main CO stripping peak on both catalysts with high carbon content shifts ca. 10–20 mV toward less positive potential

Please cite this article as: Borbáth I et al., CO tolerant Pt electrocatalysts for PEM fuel cells with enhanced stability against electrocorrosion, International Journal of Hydrogen Energy, https://doi.org/10.1016/j.ijhydene.2020.08.002

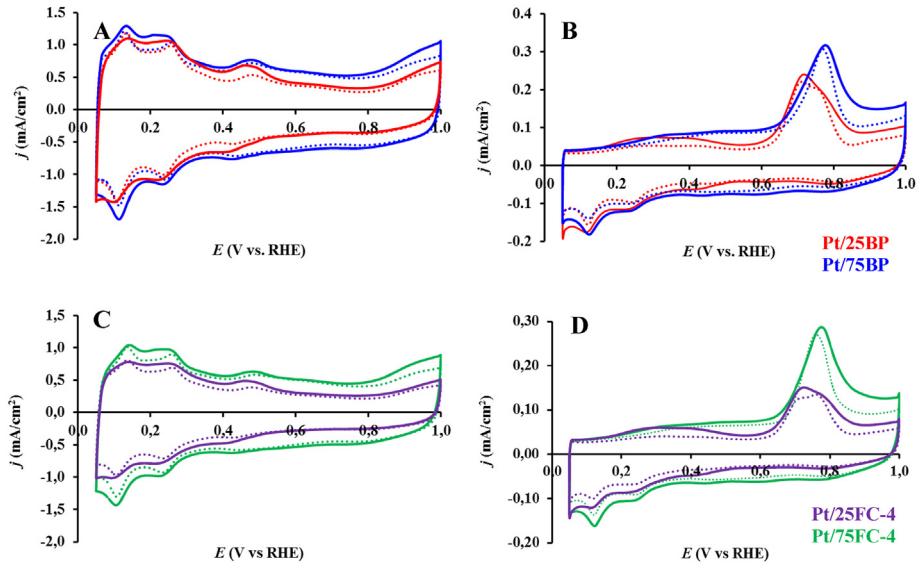

Fig. 8 – Influence of the $Ti_{0.8}Mo_{0.2}O_2$/C ratios in composite materials prepared using BP and FC-4 carbon on the electrochemical performance of the catalysts. Cyclic voltammograms (A, C) and CO_{ads} stripping voltammograms (B, D) of the electrocatalysts recorded in 0.5 M H_2SO_4 before (solid curves) and after 500 cycles (dotted curves) of the stability test. Catalysts obtained using (A, B) unmodified BP carbon (Pt/25BP (red), Pt/75BP (blue)) and (C, D) FC-4 carbonaseous material (Pt/25FC-4 (violet), Pt/75FC-4 (green)) for the preparation of composites. Sweep rate: 100 mV/s (A, C) and 10 mV/s (B, D). (For interpretation of the references to colour in this figure legend, the reader is referred to the Web version of this article.)

values in comparison to that obtained over fresh samples; on the Pt/75FC-4 catalyst this shift is more pronounced.

The electrochemically active Pt surface area (ECSA) of the electrocatalysts presented in Table 5 was calculated from the charge transfer accompanying the hydrogen desorption, taking also into account the capacitive currents, originated from double layer charging of the CVs. The loss in ECSA (Δ ECSA = $\{1\text{-}(ECSA_{500}/ECSA_1)\} \times 100\%$) was calculated from the ECSA values obtained in the 1st and 500th cycles. In the case of the Mo-containing composite supported Pt catalysts the difficulty in the precise ECSA calculation is the overlap of the Mo-related redox peaks between 380 mV and 530 mV with the under-potentially deposited hydrogen adsorption/desorption peaks. In case of the composite materials with different $Ti_{0.8}Mo_{0.2}O_2$/C ratios the second error source in the ECSA calculation is associated with the pronounced change of the charge originated from the double layer. As shown in Figs. 7 and 8 increase of the content of carbonaceous materials in the composites from 25 to 75 wt% results in a pronounced increase of the double layer charging. Upon comparison of the cyclic voltammograms presented on Fig. 8A and the ECSA values obtained on the Pt/25BP and Pt/75BP catalysts (see Table 5) this effect and its influence on the ECSA calculation can be well assessed.

The electrochemical stability tests for 500 polarization cycles performed on the catalysts studied in this work revealed that small and quite similar performance loss (Δ ECSA) was observed. The minimal difference observed on the catalysts (see Table 5) is mainly related to the accuracy of the ECSA values calculation especially taking into account the decrease of the double layer charging during the stability test (compare CV curves obtained before and after 500 cycles of the stability test on Figs. 7A,C and 8A,C).

The functionalization of carbon and using high mixed oxide content resulted in significant decrease of the specific surface area of the composite support and the ECSA value of corresponding Pt catalyst (see sample Pt/25FC-4 in Table 5). Moreover, as was already mentioned above, high oxide content in the catalyst layer can lead to a slight increase of the cell resistance and, as a consequence, to a performance loss. According to the results of the electrochemical stability test for 500 polarization cycles the Pt/75FC-4 catalyst with $Ti_{0.8}Mo_{0.2}O_2$/C ratios of 25/75 seems to be more promising.

Conclusions

Using commercial **BP** carbon and **FC** materials the sol-gel-based multistep synthesis was successfully elaborated for the preparation of the $Ti_{0.8}Mo_{0.2}O_2$–C composite supports with different mixed oxide to carbon ratios. FC materials with oxygen-containing functional groups were prepared using either a one-step treatment with glucose or by a two-step treatment with HNO_3 and glucose. Based on the results of the study of carbon functionalization treatment carried out by TG and XPS measurements, it can be concluded that:

(i) the amount and type of the surface oxygen groups depends on the type of the oxidizing/functionalizing reagent used;
(ii) treatment with glucose resulted only in the formation surface groups, which decomposed below 500 °C;

Please cite this article as: Borbáth I et al., CO tolerant Pt electrocatalysts for PEM fuel cells with enhanced stability against electrocorrosion, International Journal of Hydrogen Energy, https://doi.org/10.1016/j.ijhydene.2020.08.002

(iii) upon treatment with (HNO_3 + glucose) functional groups of different character were obtained;
(iv) upon treatment in nitrogen at 500 °C functional groups unstable at HTT can be removed;
(v) annealing of carbon at 1000 °C followed by functionalization resulted in the highest content of oxygen-containing functional groups.

XRD measurements after the deposition of the $Ti_{0.8}Mo_{0.2}O_2$ mixed oxide confirmed the lack of segregated molybdenum oxides. TEM and XPS studies indicated the success of TiO_2-based coating formation over the carbon. The decrease of the S_{BET} of the composites prepared using FCs, independently on the content of carbonaceous material, can be an indication of the formation of more homogeneous mixed-oxide coating comparing to the samples prepared using unmodified BP.

The electrochemical stability tests for 500 polarization cycles performed on the catalysts studied in this work revealed that only small performance losses (Δ ECSA) were observed. Due to the fact that high oxide content in the catalyst layer can lead to a slight increase of the cell resistance, the Pt/75FC-4 catalyst with $Ti_{0.8}Mo_{0.2}O_2$/C = 25/75 ratio seems to be more promising. However, on the Pt/25BP and Pt/25FC-4 catalysts with high mixed oxide content electrooxidation of the strongly adsorbed CO started at less positive potentials, thus demonstrating increased tolerance to CO compared to the catalysts with high carbon content.

Declaration of competing interest

The authors declare that they have no known competing financial interests or personal relationships that could have appeared to influence the work reported in this paper.

Acknowledgements

The research within project No. VEKOP-2.3.2-16-2017-00013 was supported by the European Union and the State of Hungary, co-financed by the European Regional Development Fund. Project No. NNE130004 has been implemented with the support provided from the National Research, Development and Innovation Fund of Hungary, financed under the TR-NN-17 funding scheme. Project No. NNE131270 has been implemented with the support provided from the National Research, Development and Innovation Fund of Hungary financed under the M-ERA.NET-2018 funding scheme. Financial support within project No. PD 132438 (National Research, Development and Innovation Fund of Hungary) is greatly acknowledged.

Appendix A. Supplementary data

Supplementary data to this article can be found online at https://doi.org/10.1016/j.ijhydene.2020.08.002.

REFERENCES

[1] Meier JC, Galeano C, Katsounaros I, Topalov AA, Kostka A, Schuüth F, Mayrhofer KJJ. Degradation mechanisms of Pt/C fuel cell catalysts under simulated start-stop conditions. ACS Catal 2012;2(5):832–43. https://doi.org/10.1021/cs300024h.
[2] Zhao J, Li X. A review of polymer electrolyte membrane fuel cell durability for vehicular applications: degradation modes and experimental techniques. Energy Convers Manag 2019;199:112022. https://doi.org/10.1016/j.enconman.2019.112022.
[3] Shahgaldi S, Hamelin J. Improved carbon nanostructures as a novel catalyst support in the cathode side of PEMFC: a critical review. Carbon 2015;94:705–28. https://doi.org/10.1016/j.carbon.2015.07.055.
[4] Mathias MF, Makharia R, Gasteiger HA, Conley JJ, Fuller TJ, Gittleman CI, Kocha SS, Miller DP, Mittelsteadt CK, Xie T, Yan SG, Yu PT. Two Fuel Cell cars in every garage? Electrochem Soc Interface 2005;14:24–35.
[5] Subban C, Zhou Q, Leonard B, Ranjan C, Edvenson HM, DiSalvo FJ, Munie S, Hunting J. Catalyst supports for polymer electrolyte fuel cells. Phil Trans R Soc A 2010;368:3243–53. https://doi.org/10.1098/rsta.2010.0116.
[6] Wang D, Subban CV, Wang H, Rus E, DiSalvo FJ, Abruña HD. Highly stable and CO-tolerant Pt/$Ti_{0.7}W_{0.3}O_2$ electrocatalyst for proton-exchange membrane fuel cells. J Am Chem Soc 2010;132:10218–20. https://doi.org/10.1021/ja102931d.
[7] Lv Q, Yin M, Zhao X, Li C, Liu C, Xing W. Promotion effect of TiO_2 on catalytic activity and stability of Pt catalyst for electrooxidation of methanol. J Power Sources 2012;218:93–9. https://doi.org/10.1016/j.jpowsour.2012.06.051.
[8] Huang SY, Ganesan P, Popov BN. Development of a titanium dioxide-supported platinum catalyst with ultrahigh stability for polymer electrolyte membrane fuel cell applications. J Am Chem Soc 2009;131:13898–9. https://doi.org/10.1021/ja904810h.
[9] Antolini E, Gonzalez ER. Polymer supports for low-temperature fuel cell catalysts. Appl Catal Gen 2009;365(1):1–19. https://doi.org/10.1016/j.apcata.2009.05.045.
[10] Zhang Z, Liu J, Gu J, Su L, Cheng L. An overview of metal oxide materials as electrocatalysts and supports for polymer electrolyte fuel cells. Energy Environ Sci 2014;7:2535–58. https://doi.org/10.1039/c3ee43886d.
[11] Elezović NR, Gajić-Krstajić LjM, Vračar LjM, Krstajić NV. Effect of chemisorbed CO on MoO_x-Pt/C electrode on the kinetics of hydrogen oxidation reaction. Int J Hydrogen Energy 2010;35:12878–87. https://doi.org/10.1016/j.ijhydene.2010.09.004.
[12] Ordóñez LC, Roquero P, Sebastian PJ, Ramírez J. CO oxidation on carbon-supported PtMo electrocatalysts: effect of the platinum particle size. Int J Hydrogen Energy 2007;32:3147–53. https://doi.org/10.1016/j.ijhydene.2006.02.035.
[13] Takabatake Y, Noda Z, Lyth SM, Hayashi A, Sasaki K. Cycle durability of metal oxide supports for PEFC electrocatalysts. Int J Hydrogen Energy 2014;39:5074–82. https://doi.org/10.1016/j.ijhydene.2014.01.094.
[14] Hu JE, Liu Z, Eichhorn BW, Jackson GS. CO tolerance of nano-architectured Pt-Mo anode electrocatalysts for PEM fuel cells. Int J Hydrogen Energy 2012;37:11268–75. https://doi.org/10.1016/j.ijhydene.2012.04.094.
[15] Huang J, Zang J, Zhao Y, Dong L, Wang Y. One-step synthesis of nanocrystalline TiO_2-coated carbon nanotube support for Pt electrocatalyst in direct methanol fuel cell. Mater Lett 2014;137:335–8. https://doi.org/10.1016/j.matlet.2014.09.051.

[16] Coromelci-Pastravanu C, Ignat M, Popovici E, Harabagiu V. TiO_2-coated mesoporous carbon: conventional vs. microwave-annealing process. J Hazard Mater 2014;278:382–90. https://doi.org/10.1016/j.jhazmat.2014.06.036.
[17] Zhang X, Zhou M, Lei L. Preparation of photocatalytic TiO_2 coatings of nanosized particles on activated carbon by AP-MOCVD. Carbon 2005;43:1700–8. https://doi.org/10.1016/j.carbon.2005.02.013.
[18] Vogel W, Timperman L, Alonso-Vante N. Probing metal substrate interaction of Pt nanoparticles: structural XRD analysis and oxygen reduction reaction. Appl Catal Gen 2010;377:167–73. https://doi.org/10.1016/j.apcata.2010.01.034.
[19] Liu X, Chen J, Liu G, Zhang L, Zhang H, Yi B. Enhanced long-term durability of proton exchange membrane fuel cell cathode by employing Pt/TiO_2/C catalysts. J Power Sources 2010;195:4098–103. https://doi.org/10.1016/j.jpowsour.2010.01.077.
[20] Bauer A, Song C, Ignaszak A, Hui R, Zhang J, Chevallier L, Jones D, Roziére J. Improved stability of mesoporous carbon fuel cell catalyst support through incorporation of TiO_2. Electrochim Acta 2010;55:8365–70. https://doi.org/10.1016/j.electacta.2010.07.025.
[21] von Kraemer S, Wikander K, Lindbergh G, Lundblad A, Palmqvist AEC. Evaluation of TiO_2 as catalyst support in Pt-TiO_2/C composite cathodes for the proton exchange membrane fuel cell. J Power Sources 2008;180:185–90. https://doi.org/10.1016/j.jpowsour.2008.02.023.
[22] Jiang ZZ, Gu DM, Wang ZB, Qu WL, Yin GP, Qian KJ. Effects of anatase TiO_2 with different particle sizes and contents on the stability of supported Pt catalysts. J Power Sources 2011;196:8207–15. https://doi.org/10.1016/j.jpowsour.2011.05.063.
[23] Kuriganova AB, Leontyev IN, Alexandrin AS, Maslova OA, Rakhmatullin AI, Smirnova NV. Electrochemically synthesized Pt/TiO_2-C catalysts for direct methanol fuel cell applications. Mendeleev Commun 2017;27:67–9. https://doi.org/10.1016/j.mencom.2017.01.021.
[24] Li Y, Liu C, Liu Y, Feng B, Li L, Pan H, Kellogg W, Higgins D, Wu G. Sn-doped TiO_2 modified carbon to support Pt anode catalysts for direct methanol fuel cells. J Power Sources 2015;286:354–61. https://doi.org/10.1016/j.jpowsour.2015.03.155.
[25] Wang YJ, Wilkinson DP, Neburchilov V, Song C, Guest A, Zhang J. Ta and Nb co-doped TiO_2 and its carbon-hybrid materials for supporting Pt-Pd alloy electrocatalysts for PEM fuel cell oxygen reduction reaction. J Mater Chem 2014;2:12681–5. https://doi.org/10.1039/c4ta02062f.
[26] Gubán D, Borbáth I, Pászti Z, Sajó IE, Drotár E, Hegedűs M, Tompos A. Preparation and characterization of novel $Ti_{0.7}W_{0.3}O_2$-C composite materials for Pt-based anode electrocatalysts with enhanced CO tolerance. Appl Catal B Environ 2015;174:455–70. https://doi.org/10.1016/j.apcatb.2015.03.031.
[27] Gubán D, Pászti Z, Borbáth I, Bakos I, Drotár E, Sajó IE, Tompos A. Design and preparation of CO tolerant anode electrocatalysts for PEM fuel cells. Period Polytech-Chem 2016;60:29–39. https://doi.org/10.3311/PPch.8227.
[28] Vass Á, Borbáth I, Pászti Z, Bakos I, Sajó IE, Németh P, Tompos A. Effect of Mo incorporation on electrocatalytic performance of Ti-Mo mixed oxide-carbon composite supported Pt electrocatalysts. React Kinet Mech Catal 2017;121:141–60. https://doi.org/10.1007/s11144-017-1155-5.
[29] Vass Á, Borbáth I, Bakos I, Pászti Z, Sajó IE, Tompos A. Novel Pt electrocatalysts: multifunctional composite supports for enhanced corrosion resistance and improved CO tolerance. Top Catal 2018;61:1300–12. https://doi.org/10.1007/s11244-018-0988-0.
[30] Vass Á, Borbáth I, Bakos I, Pászti Z, Sáfrán G, Tompos A. Stability issues of CO tolerant Pt-based electrocatalysts for polymer electrolyte membrane fuel cells: comparison of Pt/$Ti_{0.8}M_{0.2}O_2$-C with PtRu/C. React Kinet Mech Catal 2019;126:679–99. https://doi.org/10.1007/s11144-018-1512-z.
[31] Gubán D, Tompos A, Bakos I, Vass Á, Pászti Z, EGy Szabó, Sajó IE, Borbáth I. Preparation of CO-tolerant anode electrocatalysts for polymer electrolyte membrane fuel cells. Int J Hydrogen Energy 2017;42:13741–53. https://doi.org/10.1016/j.ijhydene.2017.03.080.
[32] Guha A, Lu W, Zawodzinski Jr TA, Schiraldi DA. Surface modified carbons as platinum catalyst support for PEM fuel cells. Carbon 2007;45(7):1506–17. https://doi.org/10.1016/j.carbon.2007.03.023.
[33] Antolini E. Carbon supports for low-temperature fuel cell catalysts. Appl Catal B: Environ 2009;88:1–24. https://doi.org/10.1016/j.apcatb.2008.09.030.
[34] Obradović MD, Vuković GD, Stevanović SI, Panić VV, Uskoković PS, Kowal A, Gojković SLj. A comparative study of the electrochemical properties of carbon nanotubes and carbon black. J Electroanal Chem 2009;634:22–30. https://doi.org/10.1016/j.jelechem.2009.07.001.
[35] Li W, Liang C, Qiu J, Zhou W, Han H, Wei Z, Sun G, Xin Q. Carbon nanotubes as support for cathode catalyst of a direct methanol fuel cell. Carbon 2002;40:791–4. https://doi.org/10.1016/S0008-6223(02)00039-8.
[36] Song H, Qiu X, Li F. Effect of heat treatment on the performance of TiO_2-Pt/CNT catalysts for methanol electro-oxidation. Electrochim Acta 2008;53:3708–13. https://doi.org/10.1016/j.electacta.2007.11.080.
[37] Duteanu N, Erable B, Senthil Kumar SM, Ghangrekar MM, Scott K. Effect of chemically modified Vulcan XC-72R on the performance of air-breathing cathode in a single-chamber microbial fuel cell. Bioresour Technol 2010:5250–5. https://doi.org/10.1016/j.biortech.2010.01.120.
[38] Aksoylu AE, Madalena M, Freitas A, Pereira MFR, Figueiredo JL. The effects of different activated carbon supports and support modifications on the properties of Pt/AC catalysts. Carbon 2001;39:175–85. https://doi.org/10.1016/S0008-6223(00)00102-0.
[39] Li L, Wu G, Xu BQ. Electro-catalytic oxidation of CO on Pt catalyst supported on carbon nanotubes pretreated with oxidative acids. Carbon 2006;44:2973–83. https://doi.org/10.1016/j.carbon.2006.05.027.
[40] Chen W, Xin Q, Sun G, Wang Q, Mao Q, Su H. The effect of carbon support treatment on the stability of Pt/C electrocatalysts. J Power Sources 2008;180:199–204. https://doi.org/10.1016/j.jpowsour.2008.02.005.
[41] Torres GC, Jablonski EL, Baronetti GT, Castro AA, de Miguel SR, Scelza OA, Blanco MD, Pena Jiménez MA, Fierro JLG. Effect of the carbon pre-treatment on the properties and performance for nitrobenzene hydrogenation of Pt/C catalysts. Appl Catal Gen 1997;161:213–26. https://doi.org/10.1016/S0926-860X(97)00071-9.
[42] de la Fuente JLG, Rojas S, Martínez-Huerta MV, Terreros P, Peña MA, Fierro JLG. Functionalization of carbon support and its influence on the electrocatalytic behaviour of Pt/C in H_2 and CO electrooxidation. Carbon 2006;44:1919–29. https://doi.org/10.1016/j.carbon.2006.02.009.
[43] Odetola C, Trevani L, Easton EB. Enhanced activity and stability of Pt/TiO_2/carbon fuel cell electrocatalyst prepared using a glucose modifier. J Power Sources 2015;294:254–63. https://doi.org/10.1016/j.jpowsour.2015.06.066.
[44] Hakamizadeh M, Afshar S, Tadjarodi A, Khajavian R, Fadaie MR, Bozorgi B. Improving hydrogen production via

Please cite this article as: Borbáth I et al., CO tolerant Pt electrocatalysts for PEM fuel cells with enhanced stability against electro-corrosion, International Journal of Hydrogen Energy, https://doi.org/10.1016/j.ijhydene.2020.08.002

water splitting over Pt/TiO_2/activated carbon nanocomposite. Int J Hydrogen Energy 2014;39:7262–9. https://doi.org/10.1016/j.ijhydene.2014.03.048.
[45] Odetola C, Trevani LN, Easton EB. Photo enhanced methanol electrooxidation: further insights into Pt and TiO_2 nanoparticle contributions. Appl Catal B Environ 2017;210:263–75. https://doi.org/10.1016/j.apcatb.2017.03.027.
[46] Odetola C, Easton EB, Trevani L. Investigation of TiO_2/carbon electrocatalyst supports prepared using glucose as a modifier. Int J Hydrogen Energy 2016;41:8199–208. https://doi.org/10.1016/j.ijhydene.2015.10.035.
[47] Fairley N. "CasaXPS: spectrum processing software for XPS, AES and SIMS," version 2.3.13. Cheshire: Casa Software Ltd; 2006. http://www.casaxps.com.
[48] Mohai M. XPS MultiQuant: multimodel XPS quantification software. Surf Interface Anal 2004;36(8):828–32.
[49] Mohai M. "XPS MultiQuant: multi-model X-ray photoelectron spectroscopy quantification program." Version 7.00.92. 2011. http://www.chemres.hu/aki/XMQpages/XMQhome.htm/.
[50] Gan L, Shang S, Yuen CWM, Jiang SX. Covalently functionalized graphene with D-glucose and its reinforcement to poly(vinyl alcohol) and poly(methyl methacrylate). RSC Adv 2015;5:15954–61. https://doi.org/10.1039/c5ra00038f.
[51] Jiang ZZ, Wang ZB, Chu YY, Gu DM, Yin GP. Carbon riveted microcapsule Pt/MWCNTs-TiO_2 catalyst prepared by in situ carbonized glucose with ultrahigh stability for proton exchange membrane fuel cell. Energy Environ Sci 2011;4:2558–66. https://doi.org/10.1039/c1ee01091c.
[52] Magon A, Pyda M. Melting, glass transition, and apparent heat capacity of α-D-glucose by thermal analysis. Carbohydr Res 2011;346(16):2558–66. https://doi.org/10.1016/j.carres.2011.08.022.
[53] Román-Martinez MC, Cazorla-Amorós D, Linares-Solano A, Salinas-Martinez de Lecea C, Yamashita H, Anpo M. Metal - support interaction in Pt/C catalysts. Influence of the support surface chemistry and the metal precursor. Carbon 1995;33:3–13. https://doi.org/10.1016/0008-6223(94)00096-I.
[54] Aksoylu AE, Freitas MMA, Figueiredo JL. Bimetallic Pt-Sn catalysts supported on activated carbon I. The effects of support modification and impregnation strategy. Appl Catal Gen 2000;192:29–42. https://doi.org/10.1016/S0926-860X(99)00330-0.
[55] de Miguel SR, Roman-Martinez MC, Jablonski EL, Fierro JLG, Cazorla-Amoros D, Scelza OA. Characterization of bimetallic PtSn catalysts supported on purified and H_2O_2-functionalized carbons used for hydrogenation reactions. J Catal 1999;184:514–25. https://doi.org/10.1006/jcat.1999.2457.
[56] Coloma E, Sepúlveda-Escribano A, Fierro JLG, Rodriguez-Reinoso F. Preparation of platinum supported on pregraphitized carbon blacks. Langmuir 1994;10:750–5. https://doi.org/10.1021/la00015a025.
[57] Coloma E, Sepúlveda-Escribano A, Fierro JLG, Rodriguez-Reinoso F. Gas phase hydrogenation of crotonaldehyde over Pt/activated carbon catalysts. Influence of the oxygen surface groups on the support. Appl Catal Gen 1997;150:165–83. https://doi.org/10.1016/S0926-860X(96)00301-8.
[58] Wagner CD, Naumkin AV, Kraut-Vass A, Allison JW, Powell CJ, Rumble Jr JR. NIST X-ray photoelectron spectroscopy database, Version 3.4. Gaithersburg, MD: National Institute of Standards and Technology; 2003. http://srdata.nist.gov/xps/.
[59] Moulder JF, Stickle WF, Sobol PE, Bomben KD. Handbook of X-ray photoelectron spectroscopy. Minnesota, USA: Perkin-Elmer Corp. Eden Prairie; 1992.
[60] Stobinski L, Lesiak B, Zemek J, Jiricek P. Time dependent thermal treatment of oxidized MWCNTs studied by the electron and mass spectroscopy methods. Appl Surf Sci 2012;258:7912–7. https://doi.org/10.1016/j.apsusc.2012.04.127.
[61] Yamada Y, Yasuda H, Murota K, Nakamura M, Sodesawa T, Sato S. Analysis of heat-treated graphite oxide by X-ray photoelectron spectroscopy. J Mater Sci 2013;48:8171–98. https://doi.org/10.1007/s10853-013-7630-0.
[62] Lazaro MJ, Celorrio V, Calvillo L, Pastor E, Moliner R. Influence of the synthesis method on the properties of Pt catalysts supported on carbon nanocoils for ethanol oxidation. J Power Sources 2011;196:4236–41. https://doi.org/10.1016/j.jpowsour.2010.10.055.
[63] Guillén-Villafuerte O, García G, Rodríguez JL, Pastor E, Guil-López R, Nieto E, Fierro JLG. Preliminary studies of the electrochemical performance of Pt/X@MoO_3/C (X= Mo_2C, MoO_2, Mo^0) catalysts for the anode of a DMFC: influence of the Pt loading and Mo-phase. Int J Hydrogen Energy 2013;38:7811–21. https://doi.org/10.1016/j.ijhydene.2013.04.083.
[64] Justin P, Rao GR. Methanol oxidation on MoO_3 promoted Pt/C electrocatalyst. Int J Hydrogen Energy 2011;36:5875–84. https://doi.org/10.1016/j.ijhydene.2011.01.122.

Please cite this article as: Borbáth I et al., CO tolerant Pt electrocatalysts for PEM fuel cells with enhanced stability against electro-corrosion, International Journal of Hydrogen Energy, https://doi.org/10.1016/j.ijhydene.2020.08.002